Received: 13 December 2022 | Revised: 12 April 2023 | Accepted: 8 May 2023

DOI: 10.1002/zamm.202200600

ZAMM

ORIGINAL PAPER

Heat transfer analysis in a curvilinear flow of hybrid nanoliquid across a curved oscillatory stretched surface with nonlinear thermal radiation

Muhammad Imran[1] | **Muhammad Naveed**[1] | **Babar Iftikhar**[2] | **Zaheer Abbas**[3]

[1]Department of Mathematics, Division of Science and Technology, University of Education, Lahore, Pakistan

[2]Department of Mathematics and Statistics, International Islamic University, Islamabad, Pakistan

[3]Department of Mathematics, The Islamia University of Bahawalpur, Bahawalpur, Pakistan

Correspondence
M. Naveed, Department of Mathematics, Division of Science and Technology, University of Education, Lahore, Pakistan.
Email: rana.m.naveed@gmail.com

The primary objective of the study is to examine the influence of the nonlinear thermal radiation on the flow of the hydromagnetic hybrid nanoliquid across an oscillating stretched curved surface. In addition, the impacts of velocity and thermal slip conditions are also considered. Curvilinear coordinate scheme is adopted to construct the mathematical form of the flow model in terms of nonlinear partial differential equations. Analytical solution of the formulated flow equations in the form of convergent series solution is accomplished by employing the Homotopy analysis technique (HAM). A comprehensive inspection of the consequences of different flow parameters, such as the hybrid nanoparticles parameter, magnetic parameter, non-dimensional velocity slip parameter, dimensionless radius of curvature, dimensionless thermal slip parameter, Prandtl number, dimensionless temperature parameter on the flow, pressure, surface drag force, temperature and on the local Nusselt number is conducted out through graphs and tables and discussed in detail. It is noticed that the amplitude of the liquid velocity is a reducing function of the solid volume fraction parameter for copper and the velocity slip parameter, whereas it is enhanced with increasing solid volume fraction parameter for alumina.

1 | INTRODUCTION

In current years, the inspection of nanoliquid dynamics has captured the remarkable attention of numerous investigators and engineers due to its prominent importance in the arena of high heat transmission mechanisms and the contemporary creation of cooling system. The types of liquids like oil, ethylene glycol, and water are commonly categorized as base liquids because of their extremely low thermal conductivity. For the improvement of the thermal conductivity of base liquids, a minuscule pinch of nanoparticles ($<1\%$) is merged in such liquids. The actual size and shape of these nanoparticles are measured very small so that they can locomote efficiently through micro channels without plugging them. With the accessibility of the author's information, Choi [1] was the first to propose the idea of the movement of nanofluids. Hayat et al. [2] has examined mixed convection motion for the copper and silver water nanoliquids above curved stretched surface. In another article, Hayat et al. [3] has considered the impacts of nonlinear velocity in motion of nanofluids across stretching wall. Abbas et al. [4] has computed the thermophoresis and Brownian motion effects on curvilinear oscillatory flow of Casson nanoliquid towards stretching sheet. For more comprehensive investigation about the nanofluids over different geometries, the reader must read the articles which are referenced [5–10] in the reference section.

The most significant category of nanoliquid, which is the result of the composition of two different types of nanoparticles in base liquid is termed as hybrid nanoliquid. The basic purpose of this type of modification in nanofluids is to grant better thermo physical features and rheological behavior along with a modified heat transport mechanism. The most imperative applications of these types of nanoliquids are in the arenas of heat transmission procedures, including microfluidics, defense, manufacturing, transportation and acoustics. Waini et al. [11] has observed the liquid motion and heat transport phenomena in hybrid nanofluid on a stretched/shrinked curved sheet. An Inspection of curvilinear hybrid based nanoliquid flow towards a stretched wall was completed by Nadeem et al. [12]. Saeed et al. [13] has performed an analytical research for Darcy-Forchheimer hybrid nanoliquid curvilinear motion over stretchable surface. Naveed et al. [14] has evaluated the impacts of melting heat transmission on hybrid nanofluid motion past across curved stretched surface. A detailed comprehensive literature about the hybrid nanofluids with different assumptions is referenced in references [15–19].

Because of its extensive physical implications in many manufacturing and technological operations, the examination of boundary layer movement towards a stretched surface has attracted the interest of many researchers and engineers now a days. Such operations involve developed of plastic sheets, condensing process, plastic foam dispensation, continuous exhausted of a sheet in metallurgical operations, generation of artificial fibers, and extrusion of polymer sheets from a die, paper production industries, textile industries, crystalline materials and glass fiber. The first assessment of the liquid motion towards a stretched sheet was performed by Crane [20]. He provided an exact solution in the closed form for the considered flow problem. After Crane [20], several investigators expanded his concept to explore the dissimilar aspects of viscous and non-Newtonian liquids over curved and flat stretching sheets by considering either linear or nonlinear velocity, exponential and oscillatory velocity. Sajid et al. [21] has examined the viscous flow phenomenon across a stretchable curved surface. Naveed et al. [22] has detected the different features of heat transmission phenomenon in magnetohydrodynamic motion on a generalized stretching or shrinking curved sheet. The inspection of heat transport analysis across nonlinear stretched curved sheet was finalized by Sanni et al. [23]. Shi et al. [24] has evaluated numerical solution for an exponential curved stretchable non-Newtonian liquid motion. Impacts of thermo diffusion and heat production on time dependent flow of chemically reactive Oldroyd-B liquid towards oscillatory moving surface was calculated by Sami et al. [25]. Abbas et al. [26] has examined the different aspects of transport of heat phenomena along with constant magnetic field in viscous liquid motion past above on stretched oscillatory curved surface. Imran et al. [27] has accomplished an analytical exploration for the motion of magneto nanoparticles towards a curved oscillatory stretching wall. Curvilinear motion of non-Newtonian micropolar fluid past over a curved oscillatory stretchable sheet with Cattaneo-Christov heat flux was researched by Naveed et al. [28]. Imran et al. [29] has considered the effects of heat and mass transportation phenomena's by considering modified Fourier and Fick's model in flow of Eyring-Powell liquid across a curved oscillating stretched sheet. Naveed et al. [30] has inspected the influences of variable thermal conductivity and diffusivity in convectively heated Williamson fluid towards an oscillatory curved Riga surface. Heat transport analysis in the chemically reactive flow of couple stress fluid towards a porous oscillatory sheet has been done by Naveed et al. [31]. Very lately, Imran et al. [32] has performed an analytical examination and investigate the Soret and Duffour effects on the oscillatory flow of couple stress liquid over a curved stretchable sheet.

The inspection of magnetohydrodynamic liquid motion with the incorporation of nonlinear thermal radiation impacts has affianced the concentration of various engineers and investigators due to its inspiring implications in the procedures of high temperature involvement, such that nuclear plants, missiles, gas turbines, satellites, storage of thermal energy, and in various propulsion devices for space vehicles. Abbas et al. [33] has calculated the consequences of thermal nonlinear radiation in hydromagnetic motion of Carreau liquid inside a curved channel. Naveed et al. [34] has conducted a numerical inquiry and calculate the effects of thermal radiation in chemically reactive Eyring-Powell fluid via a semi-permeable curved channel. In another article, Naveed et al. [35] has computed the effects of thermal radiation and entropy optimization on curvilinear flow of viscous liquid towards curved oscillating Riga surface.

In many technological and industrial procedures, like internal cavities and polishing artificial heart valves, the effects of velocity and thermal slip conditions are very dominant. Abbas et al. [36] has studied impacts of heat production in hydromagnetic slip flow of nanoliquid towards curved stretched wall. Meenakumari et al. [37] has detected the influences of slip conditions and constant magnetic field in chemically reactive flow over stretching sheet. Wahid et al. [38] has inspected magnetohydrodynamic slip Darcy flow of viscoelastic liquid with thermal radiation impacts past over stretching sheet.

The prime focus of the present article is to discuss the consequences the nonlinear thermal radiation on the flow of hybrid nanoliquid across a curved stretched oscillatory surface in presence of magnetic field. Furthermore, the impacts of velocity slip parameter to the flow and thermal slip condition to the heat transfer are also considered. A literature survey reveals that no one has yet discussed the influence of non-linear thermal radiation on the hybrid nanofluid over the oscillating curved stretching surface in presence of applied magnetic field. The devolved partial differential equations describing the flow phenomena are then solved analytically via Homotopy analysis method (HAM) [26]. The

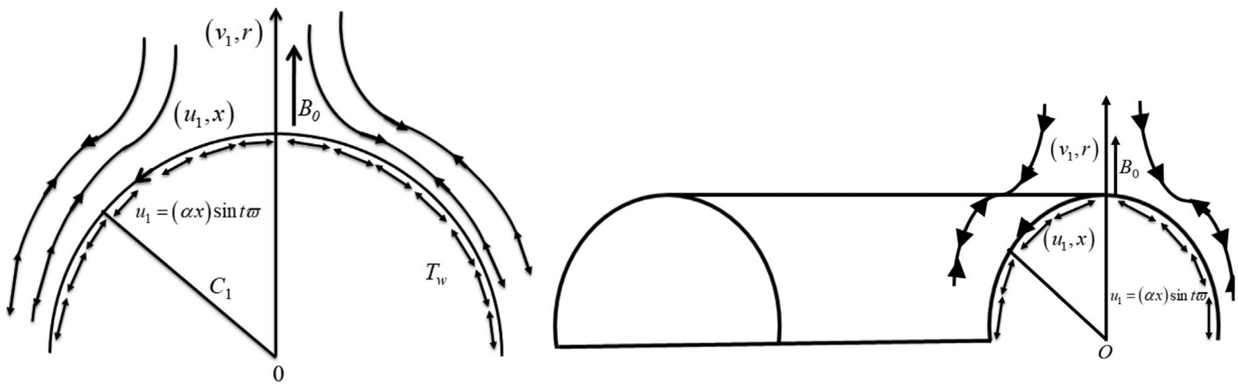

FIGURE 1 Schematic flow geometry.

influences of related variables on pressure, skin friction, velocity, local Nusselt number, and temperature are exposed via tables and graphs and discussed in detail. For the authentication of contemporary article, comparative analysis are also accomplished and achieved in admirable agreement. Furthermore, this research work is original and has not yet been published anywhere else.

2 | PROBLEM INTERPRETATION

Consider two dimensional and time-dependent boundary layer movement of an electrically conducting hybrid nanoliquid across a stretched curved oscillatory sheet warped in the nature of semicircle with radius C_1 (see Figure 1).The liquid motion is occurred by the periodic fluctuation of an elastic sheet along the axial direction x. Let $u_1 = (\alpha x)\sin t\varpi$ be the oscillating stretched velocity of the sheet with ϖ is the oscillatory frequency and α is the stretched rate constant. Also, a constant magnetic field of strength B_0 is implemented along the radial direction x. The influence of induced magnetic field can be ignored by considering very low magnetic Reynolds number assumptions. Let T_∞ and T_w be the ambient and sheet temperature with $(T_w > T_\infty)$.

In view of the foresaid assumptions the governing equations for the given problem can be written as [5, 35].

$$C_1\frac{\partial u_1}{\partial x} + \frac{\partial}{\partial r}\{(C_1 + r)\, v_1\} = 0, \tag{1}$$

$$\frac{1}{\rho_{hnf}}\frac{\partial p}{\partial r} = \frac{{u_1}^2}{C_1 + r}, \tag{2}$$

$$\begin{aligned}\frac{\partial u_1}{\partial t} + v_1\frac{\partial u_1}{\partial r_1} + \frac{u_1 v_1}{C_1 + r} + \frac{C_1 u_1}{C_1 + r}\frac{\partial u_1}{\partial x} &= -\frac{1}{\rho_{hnf}}\frac{C_1}{C_1 + r}\frac{\partial p}{\partial x}\\ &+\frac{\mu_{hnf}}{\rho_{hnf}}\left(\frac{\partial^2 u_1}{\partial r^2} - \frac{u_1}{(C_1 + r)^2} + \frac{1}{C_1 + r}\frac{\partial u_1}{\partial r}\right) - \frac{\sigma_{hnf}}{\rho_{hnf}}B_0^2 u_1,\end{aligned} \tag{3}$$

$$\left(\frac{\partial T}{\partial t} + \frac{C_1 u_1}{C_1 + r}\frac{\partial T}{\partial x} + \frac{\partial T}{\partial r}v_1\right) = \frac{k_{hnf}}{(\rho c_p)_{hnf}}\left(\frac{\partial^2 T}{\partial r^2} + \frac{1}{C_1 + r}\frac{\partial T}{\partial r}\right) - \frac{1}{(\rho c_p)_{hnf}(C_1 + r)}\frac{\partial}{\partial r}\left((C_1 + r)\,\widehat{q}_r\right) = 0, \tag{4}$$

With associated boundary conditions

$$\left.\begin{aligned}&v_1 = 0, \quad u_1 = (\alpha\, x)\; sin\, t\varpi + \ell_1\left(\tfrac{\partial u_1}{\partial r} - \tfrac{u_1}{C_1 + r}\right), \quad T = T_w + \ell_2\tfrac{\partial T}{\partial r}, \ \text{ at } r = 0,\\ &\tfrac{\partial u_1}{\partial r} \to 0, \quad u_1 \to 0, \ T \to T_\infty, \quad \text{at } r \to \infty.\end{aligned}\right\} \tag{5}$$

Here u_1 is the velocity part along axial x- direction, p and T are the pressure and temperature of the fluid, v_1 is the velocity part in r- direction, ℓ_1 is the velocity slip parameter, and ℓ_2, ρ_{hnf}, $\widehat{q}_r$, σ_{hnf}, k_{hnf} and μ_{hnf} are thermal slip

TABLE 1 The physical properties for $\mu_{hnf}, \rho_{hnf}, k_{hnf}$ are given in Naveed et al. [14].

Properties	Nanofluid	Hybrid nanofluid
Density	$\rho_{nf} = \rho_{s1}\varphi_1 + (1-\varphi_1)\rho_f$	$\rho_{hnf} = (1-\varphi_2)(\rho_{s1}\varphi_1 + \rho_f(1-\varphi_1)) + \rho_{s2}\varphi_2$
Heat capacity	$(\rho c_p)_{nf} = -(\varphi_1+1)(\rho c_p)_f + \varphi_1(\rho c_p)_{s1}$	$(\rho c_p)_{hnf} = \varphi_2(\rho c_p)_{s2} - (\varphi_2-1)((\rho c_p)_f(1-\varphi_1) + \varphi_1(\rho c_p)_{s1})$,
Dynamic viscosity	$\mu_{nf} = \frac{\mu_f}{(1-\varphi_1)^{2.5}}$	$\mu_{hnf} = \frac{\mu_f}{(1-\varphi_1)^{2.5}(1-\varphi_2)^{2.5}}$
Thermal conductivity	$\frac{k_{nf}}{k_f} = \frac{2k_f+k_{s1}-2\varphi_1(k_f-k_{s1})}{2k_f+k_{s1}+(k_f-k_{s1})\varphi_1}$	$\frac{k_{hnf}}{k_{nf}} = \frac{2k_{nf}+k_{s2}-2\varphi_2(k_{nf}-k_{s2})}{2k_{nf}+k_{s2}+(k_f-k_{s2})\varphi_1}$
Electrical conductivity	$\frac{\sigma_{nf}}{\sigma_f} = \frac{(1+2\varphi_1)\sigma_{s1}-2\sigma_f(\varphi_1-1)}{(1-\varphi_1)\sigma_{s1}+\sigma_f(2+\varphi_1)}$	$\frac{\sigma_{hnf}}{\sigma_{nf}} = \frac{(1+2\varphi_2)\sigma_{s2}+2\sigma_{nf}(1-\varphi_2)}{(1-\varphi_2)\sigma_{s2}+\sigma_{nf}(2+\varphi_2)}$

TABLE 2 Physical properties of nanofluid Naveed et al. [14].

Properties	ρ	c_p	$\beta \times 10^5$	k	σ
Base fluid	997.1	4179	21	0.613	0.05
Alumina (Al_2O_3)	3970	765	0.85	40	10^{-10}
Copper (Cu)	8933	385	1.67	401	5.96×10^7

parameter, density, radiative heat flux, electrical conductivity, thermal conductivity and viscosity of the hybrid nanoliquid respectively.

The thermo physical properties for both nanoliquid and hybrid liquid is given in Table 1.

Whereas the physical properties of the base fluid (water), Al_2O_3 (alumina) and Cu (copper) are given in Table 2.

The expression for radiative heat flux in terms of Rosseland approximation is defined as

$$\widehat{q}_r = -\frac{4\widehat{\sigma}}{3\widehat{k}_\gamma}\frac{\partial T^4}{\partial r} = -\frac{16\widehat{\sigma}}{3\widehat{k}_\gamma}T^3\frac{\partial T}{\partial r}, \tag{6}$$

In above equation $\widehat{\sigma}$ expresses the Stefan-Boltzmann constant and $\widehat{k}_\gamma$ represents the absorption coefficient, and which is nonlinear in T.

Invoking Equation (6), the energy Equation (4) yields

$$\frac{\partial T}{\partial t} + \frac{C_1 u}{C_1+r}\frac{\partial T}{\partial x} + \frac{\partial T}{\partial r}v_1 = \frac{k_{hnf}}{(\rho c_p)_{hnf}}\left(\frac{\partial^2 T}{\partial r^2} + \frac{1}{C_1+r}\frac{\partial T}{\partial r}\right) + \frac{1}{(\rho c_p)_{hnf}(C_1+r)}\frac{\partial}{\partial r}\left((C_1+r)\left(\frac{16T^3\widehat{\sigma}}{3\widehat{k}_\gamma}\right)\right) = 0, \tag{7}$$

Incorporating the following dimensionless variables

$$\sqrt{\frac{\alpha}{\nu_f}}r = \xi,\ \alpha x F_\xi(\xi,\tau) = u_1,\ \frac{-C_1}{C_1+r}\sqrt{\alpha\nu_f}F(\xi,\tau) = v_1,$$
$$t\varpi = \tau,\ \rho_f\alpha^2 x^2 P(\xi,\tau) = p,\ \ T = T_\infty - (T_\infty - T_w)\theta(\xi,\tau). \tag{8}$$

Making use of Equation (8), Equation (1) is identically verified, and Equations (2), (3), (5), and (7) yield

$$\frac{\partial P}{\partial \xi} = \frac{A_{12}{F_\xi}^2}{\delta+\xi}, \tag{9}$$

$$P(\xi,\tau) = \frac{\delta+\xi}{2\delta}\left(\begin{array}{l}\frac{A_{12}}{A_{11}}\left(F_{\xi\xi\xi} + \frac{F_{\xi\xi}}{(\delta+\xi)} - \frac{F_\xi}{(\delta+\xi)^2}\right) - \frac{\sigma_{hnf}}{\sigma_f}F_\xi M^2 \\ +A_{12}\left(\frac{\delta}{(\delta+\xi)}F F_{\xi\xi} - F_\xi^2\frac{\delta}{(\delta+\xi)} + \frac{F F_\xi \delta}{(\delta+\xi)^2} - SF_{\xi\tau}\right)\end{array}\right), \tag{10}$$

$$\frac{k_{hnf}}{PrA_{13}k_f(\delta+\xi)}\frac{\partial}{\partial\xi}\left(\left(1+\frac{k_f}{k_{hnf}}\lambda(1+(\theta_w-1)\theta)^3\right)(\delta+\xi)\theta_\xi\right)+\left(\frac{\delta}{(\delta+\xi)}F\theta_\xi-S\theta_\tau\right)=0, \tag{11}$$

$$\theta(0,\tau)=1+\Gamma\theta_\xi(0,\tau),\ \ F(0,\tau)=0,\ \ F_\xi(0,\tau)=sin\tau+\gamma\left(F_{\xi\xi}(0,\tau)-\frac{1}{\delta}F_\xi(0,\tau)\right),$$
$$F_\xi(\infty,\tau)=0,\quad \theta(\infty,\tau)=0,\quad F_{\xi\xi}(\infty,\tau)=0, \tag{12}$$

where $\delta(=C_1\sqrt{\alpha/\nu_f})$ express the dimensionless parameter of curvature, $Pr(=\nu_f/\alpha_f)$ the Prandtl number, $\gamma(=\ell_1\sqrt{\alpha/\nu_f})$ the dimensionless velocity slip parameter, $S(=\varpi/\alpha)$ the proportion of periodic frequency of the sheet to stretched rate, $\Gamma(=\ell_2\sqrt{\alpha/\nu_f})$ the dimensionless thermal slip parameter, $M^2(=\sigma_f B_0^2/\rho_f\alpha)$ the magnetic parameter, $\theta_w(=T_w/T_\infty)$ the dimensionless temperature parameter and $\lambda(=16\widehat{\sigma}T_\infty^3/3\widehat{k}_\gamma k_f)$ the radiation parameter.

The liquid velocity equation can be accomplished after extrusion of pressure from the Equations (9) and (10) as

$$F_{\xi\xi\xi\xi}+\frac{2}{(\delta+\xi)}F_{\xi\xi\xi}-\frac{F_{\xi\xi}}{(\delta+\xi)^2}+\frac{F_\xi}{(\delta+\xi)^3}-\frac{A_{11}}{A_{12}}\left(F_{\xi\xi}+\frac{F_\xi}{\delta+\xi}\right)\frac{\sigma_{hnf}}{\sigma_f}M^2$$
$$+A_{11}\left(-\frac{\delta\left(F_\xi F_{\xi\xi}-FF_{\xi\xi\xi}\right)}{(\delta+\xi)}+\frac{\delta FF_{\xi\xi}}{(\delta+\xi)^2}-\frac{FF_\xi\delta}{(\delta+\xi)^3}-\frac{F_\xi^2\delta}{(\delta+\xi)^2}-F_{\xi\xi\tau}S-\frac{SF_{\xi\tau}}{\delta+\xi}\right)=0. \tag{13}$$

where

$$A_{11}=(-\varphi_2+1)^{2.5}(-\varphi_1+1)^{2.5}\left((-\varphi_2+1)\left((-\varphi_1+1)+\varphi_1\left(\rho_{s1}/\rho_f\right)\right)+\varphi_2\left(\rho_{s2}/\rho_f\right)\right), \tag{14}$$

$$A_{12}=-(\varphi_2-1)\left(\varphi_1\left(\rho_{s1}/\rho_f\right)+(-\varphi_1+1)\right)+\varphi_2\left(\rho_{s2}/\rho_f\right), \tag{15}$$

$$A_{13}=(-\varphi_2+1)\left((-\varphi_1+1)+\left((\rho c_p)_{s1}/(\rho c_p)_f\right)\varphi_1\right)+\varphi_2\left((\rho c_p)_{s2}/(\rho c_p)_f\right), \tag{16}$$

The substantial quantities such as heat transport rate and surface drag force in the $x-$ direction are

$$C_F=\frac{\tau_{rx}}{\rho u_w^2},\quad Nu_x=\frac{xq_w}{(T_w-T_\infty)k_f}, \tag{17}$$

where τ_{rx} and q_w are depicted as

$$\tau_{rx}=-\mu_{hnf}\left(\frac{u_1}{C_1+r}-\frac{\partial u_1}{\partial r}\right)\Big|_{x=0},\quad q_w=-\left(k_{hnf}\frac{\partial T}{\partial r}\right)\Big|_{x=0}, \tag{18}$$

Using Equation (8) in Equations (17) and (18), we get

$$\sqrt{Re_x}C_F=\frac{1}{(1-\varphi_1)^{2.5}(1-\varphi_2)^{2.5}}\left(F_{\xi\xi}(0,\ \tau)-\frac{F_\xi(0,\tau)}{\delta}\right), \tag{19}$$

$$\frac{Nu_x}{\sqrt{Re_x}}=-\frac{k_{hnf}}{k_f}\left(1+\frac{k_f}{k_{hnf}}Rd(1+(\theta_w-1)\theta)^3\right)\theta_\xi(0,\tau). \tag{20}$$

TABLE 3 Comparison of $F''(0,\tau)$ for unalike values of τ when $S = 1.0$, $\varphi_1 = 0, M = 12, \varphi_2 = 0$ and $\delta_1 \to \infty$.

τ	Sami et al. [25]	Abbas et al. [26]	Current results
$\tau = 3\pi/2$	11.678656	11.678656	11.678656
$\tau = 11\pi/2$	11.678707	11.678706	11.678706
$\tau = 19\pi/2$	11.678656	11.678656	11.678656

3 | EXPLANATION OF SOLUTION METHODOLOGY BY HAM

The main motive of this segment is to explain the HAM which we have utilized to compute the convergence series solution of Equations (11) and (13) with appropriate boundary conditions given in Equation (12) by considering following expressions

$$\theta_0(\xi,\tau) = \frac{1}{(\lambda+1)} exp(-\xi), \quad F_0(\xi,\tau) = \frac{sin\tau}{\left(1+\kappa\left(1+\frac{1}{\delta}\right)\right)}(-exp(-\xi)+1), \tag{21}$$

$$Q_\theta(\theta) = \frac{\partial^2\theta}{\partial\xi^2} - \theta, \quad Q_F(F) = \frac{\partial^4 F}{\partial\xi^4} - \frac{\partial^3 F}{\partial\xi^3} - \frac{\partial^2 F}{\partial\xi^2} + \frac{\partial F}{\partial\xi}, \tag{22}$$

Which satisfying the following results

$$\begin{aligned} &Q_F\left[(B_2 + B_3\xi) exp(\xi) + B_4 exp(-\xi) + B_1\right] = 0,\\ &Q_\theta\left[B_5 exp(\xi) + B_6 exp(-\xi)\right] = 0. \end{aligned} \tag{23}$$

where, B_i $(i = 1,2,3,4,5,6)$ are representing the arbitrary constants.

4 | DISCUSSION OF ANALYTICAL RESULTS

This segment significance the effects of numerous concerned physical parameters likely velocity slip parameter (γ), dimensionless form radius of curvature parameter (δ), thermal slip parameter (Γ), magnetic parameter (M), radiation parameter (λ), dimensionless temperature parameter (θ_w), variable of solid volume fraction for Alumina (φ_1), the fraction of parameter of oscillation of the wall to its stretched rate (S), Prandtl number (Pr) and solid volume fraction parameter for Copper (φ_2) on profile $F'(\xi,\tau)$, $P(\xi,\tau)$ distribution, skin friction coefficient $(\sqrt{\mathrm{Re}_x}C_F)$, temperature distribution $\theta(\xi,\tau)$ and on Nusselt number $(Nu_x/\sqrt{\mathrm{Re}_x})$ via graphical and tabular form in detail.

Table 3 is drawn to check the validity of the current study by comparing existing results in the literature [25, 26] as a special case for flat and curved oscillatory surfaces, and finding excellent agreement. Table 4 presents the variation in arithmetic values of $(Nu_x/\sqrt{\mathrm{Re}_x})$ for distinct values of $(\delta), (\varphi_1), (\varphi_2), (\lambda), (Pr), (\theta_w)$ and (Γ). This table remarked that the magnitude of $(Nu_x/\sqrt{\mathrm{Re}_x})$ reduces for advanced values of $(\delta), (\Gamma), (\varphi_1)$ and it is enlarged with a growth in $(\varphi_2), (\lambda), (\theta_w)$ and (Pr).

Figure 2a-d is made to investigate the impacts of dissimilar parameter (δ), (φ_1), (φ_2) and (γ) on the profile $F'(\xi,\tau)$. This figure verifies that amplitude of $F'(\xi,\tau)$ diminishes with mounting values of the parameters of radius of curvature (δ), solid volume fraction parameter (φ_2) and velocity slip parameter (γ) and is enhanced with growing values of (φ_1). Figure 3a-d shows the consequences of (δ), (φ_1), (φ_2) and (γ) on $F'(\xi,\tau)$ at $\tau = \pi/2$ fixed. From these figures it is clearly observed that $F'(\xi,\tau)$ rises for upward values of (δ) and (φ_1) and it declines with higher values of (φ_2) and (γ). This is due to the presence of slip, the flow velocity near the curved surface is no longer equal to the oscillatory stretched velocity of the curved surface. Therefore, with growing values of the slip parameter, slip velocity increases, and consequently, the liquid velocity diminishes because the slip condition will affect the momentum of the oscillatory stretched surface to the fluid.

Figure 4a-d witnessed that the amplitude of $P(\xi,\tau)$ shows decreasing response with all parameters (φ_1), $(S), (\varphi_2)$ and (γ). The change in $P(\xi,\tau)$ at $\tau = \pi/2$ under the influences of (φ_1), $(\varphi_2), (\gamma)$ and (S) is explained through Figure 5a-d. One can detected from Figure 5a-d that pressure distribution $P(\xi,\tau)$ is declined with increasing (φ_1), $(\varphi_2), (\gamma)$ and (S).

Figure 6a-d portrays the results of diverse factors like $(\delta), (\varphi_1)$, $(\varphi_2), (\lambda), (\mathrm{Pr})$, (θ_w) and (Γ) on the temperature profile $\theta(\xi,\tau)$ respectively at $\tau = \pi/2$ fixed. This figure depicts that the temperature of the hybrid nanofluid is mounting function

TABLE 4 Assessment values of $(Nu_x/\sqrt{\mathrm{Re}_x})$ for some values of $(\delta), (\varphi_1), (\varphi_2), (\lambda), (Pr), (\theta_w)$ and (Γ) with $M = 0.1, S = 0.5$ and $\gamma = 0.2$ fixed.

δ	φ_1	φ_2	λ	Pr	θ_w	Γ	$Nu_x/\sqrt{\mathrm{Re}_x}$
1.0	0.02	0.02	0.5	1.0	0.5	0.1	1.02976
2.0							1.02412
3.0							1.01849
1.0	0.01						1.02988
	0.05						1.02897
	0.09						1.02784
	0.02	0.01					1.00226
		0.03					1.05781
		0.05					1.11562
		0.02	1.0				1.10111
			1.5				1.17219
			2.0				1.24301
			0.5	2.0			1.03089
				3.0			1.03203
				4.0			1.03316
				1.0	0.4		0.97855
					0.6		1.07270
					0.8		1.20354
					0.5	0.2	0.95947
						0.3	0.89930
						0.4	0.84699

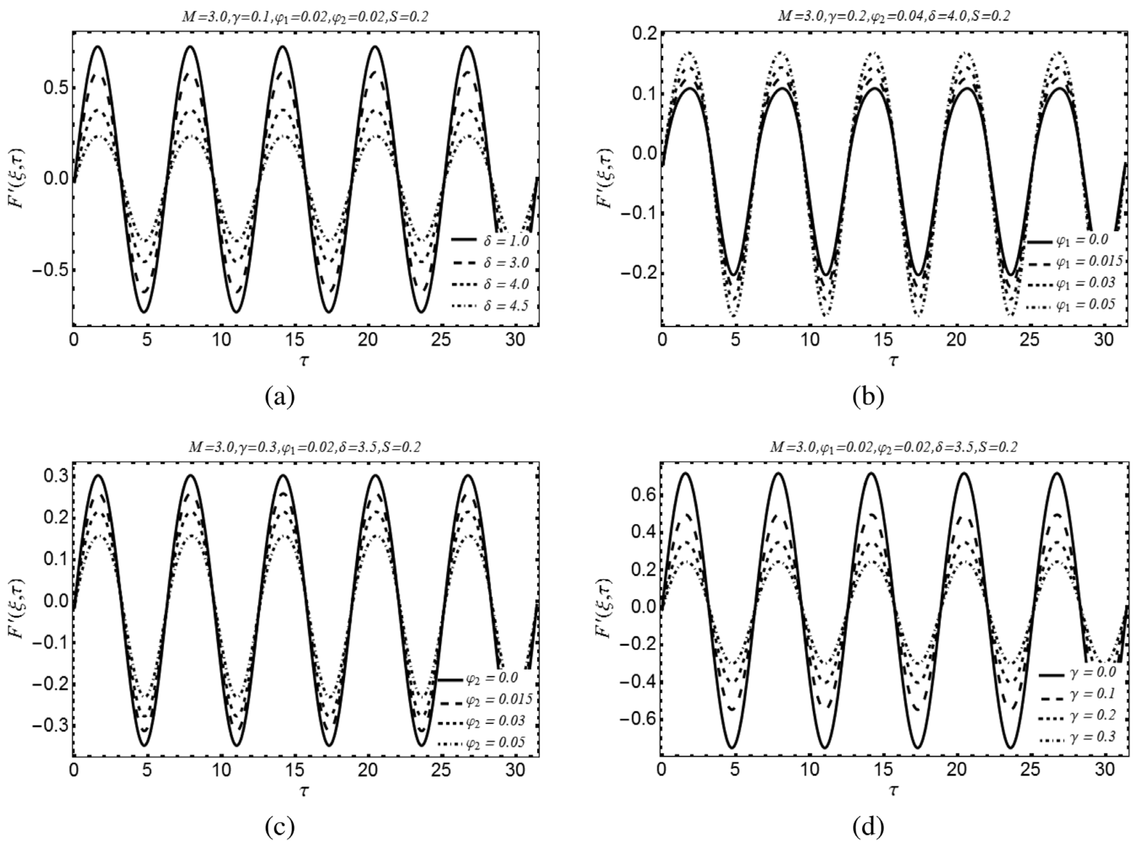

FIGURE 2 Consequences of dissimilar variables on $F'(\xi, \tau)$.

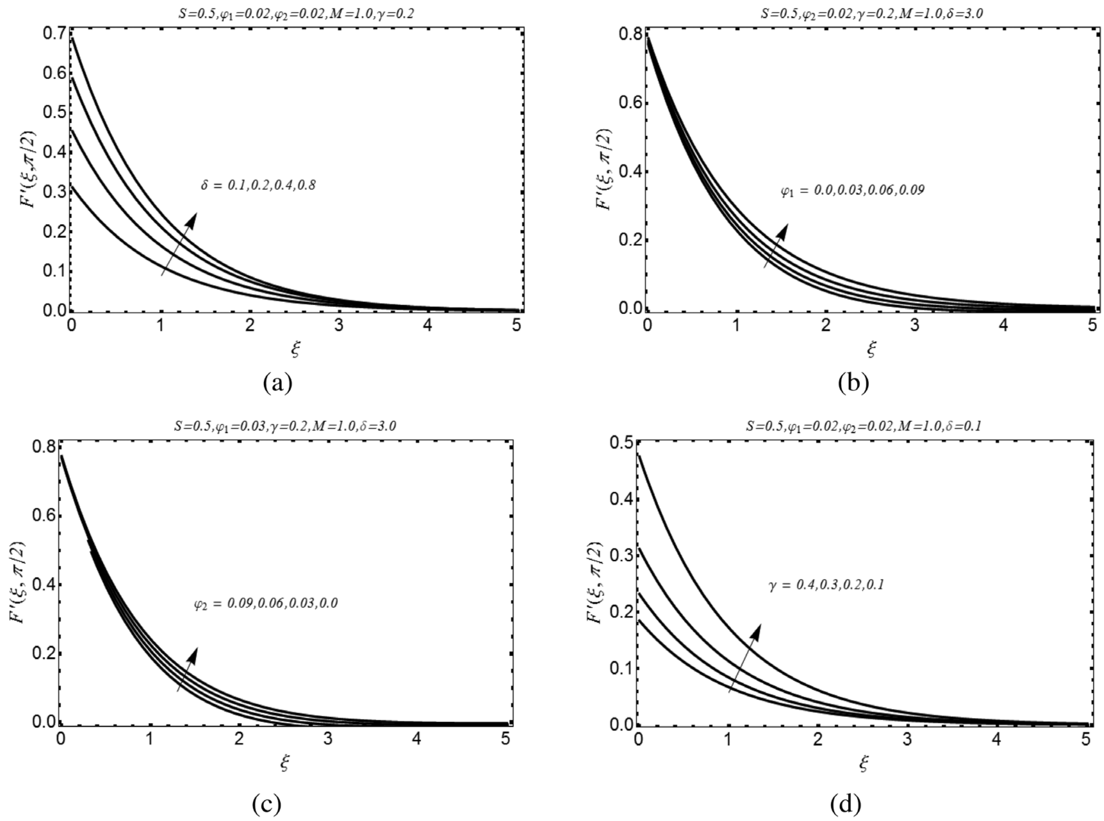

FIGURE 3 Alteration of dislike concerned flow variables on profile $F'(\xi,\tau)$ at $\tau = \pi/2$.

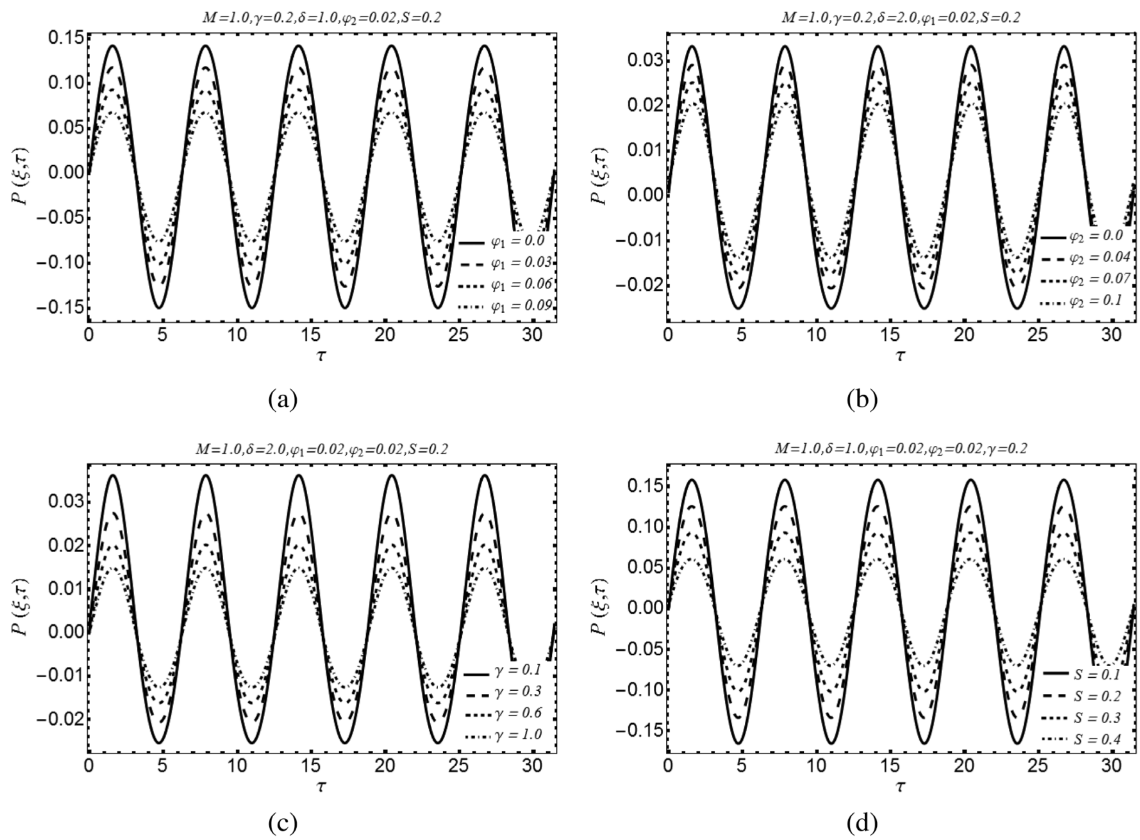

FIGURE 4 Variation in distribution $P(\xi,\tau)$.

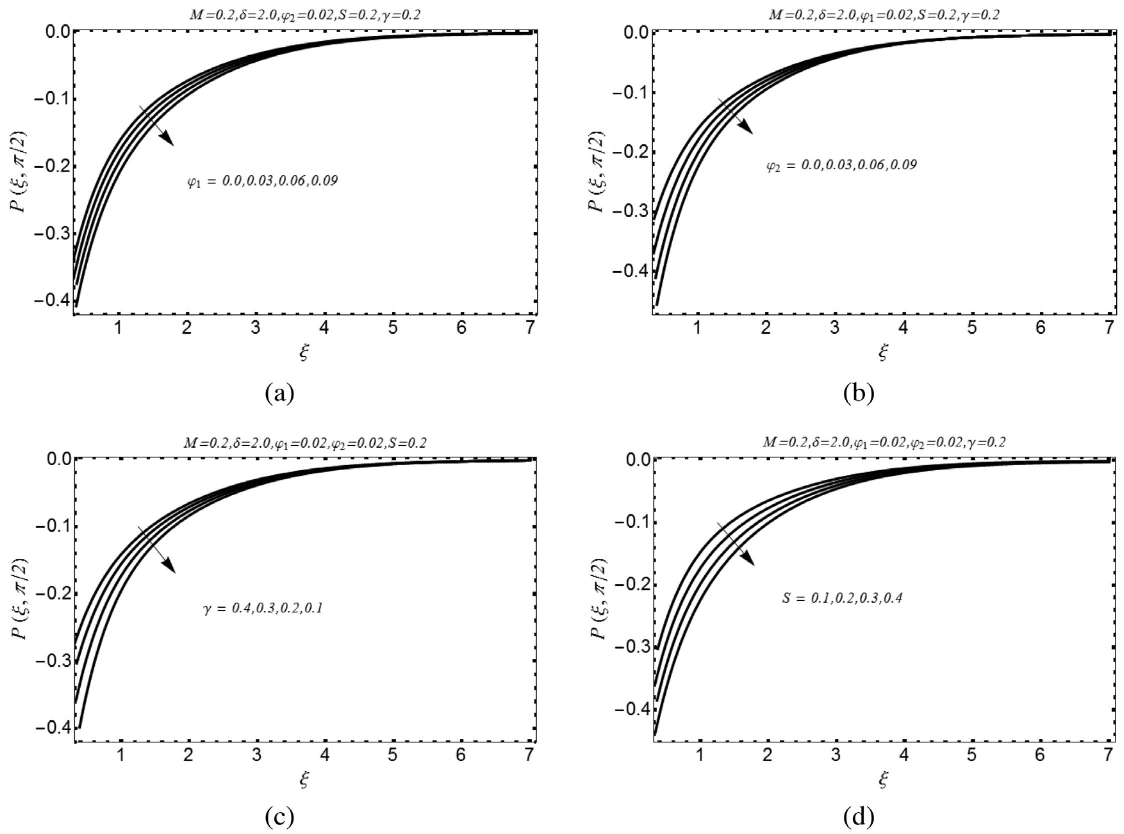

FIGURE 5 Variation in pressure distribution $P(\xi, \tau)$.

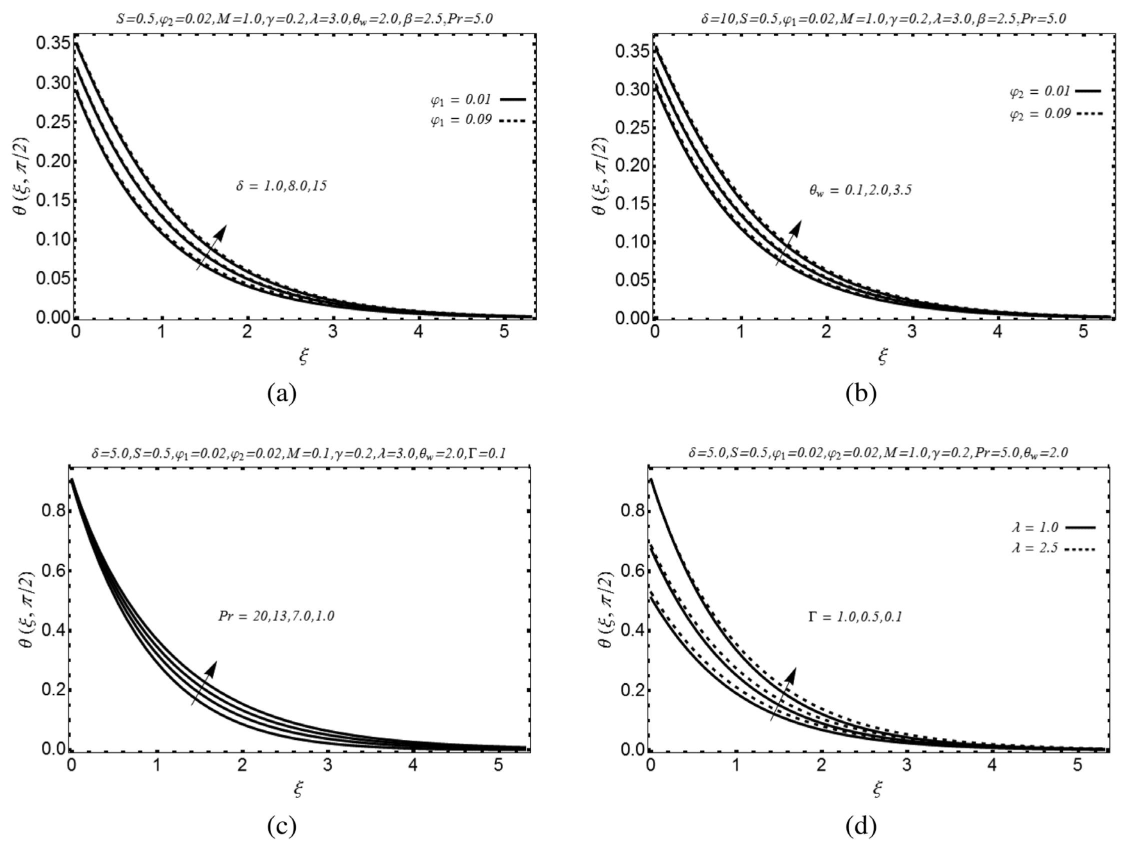

FIGURE 6 Variation in profile $\theta(\xi, \tau)$.

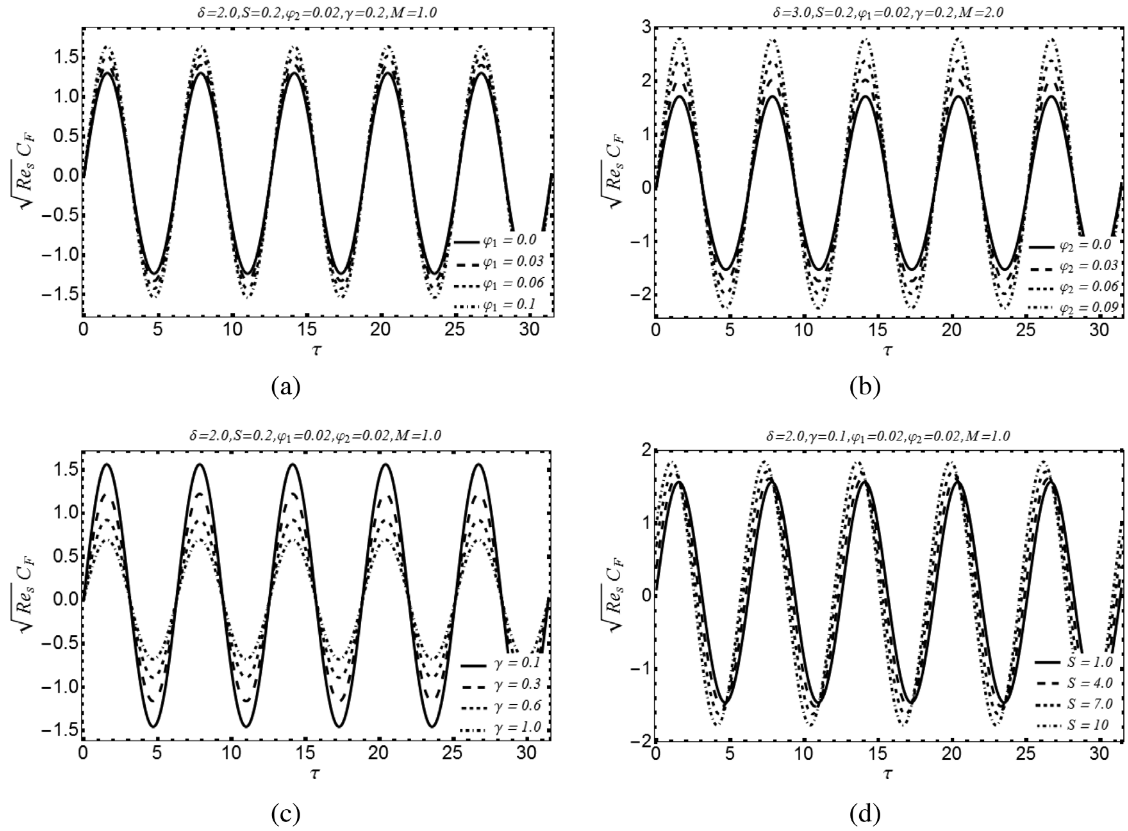

FIGURE 7 Variation in skin friction coefficient $\sqrt{Re_x}C_F$.

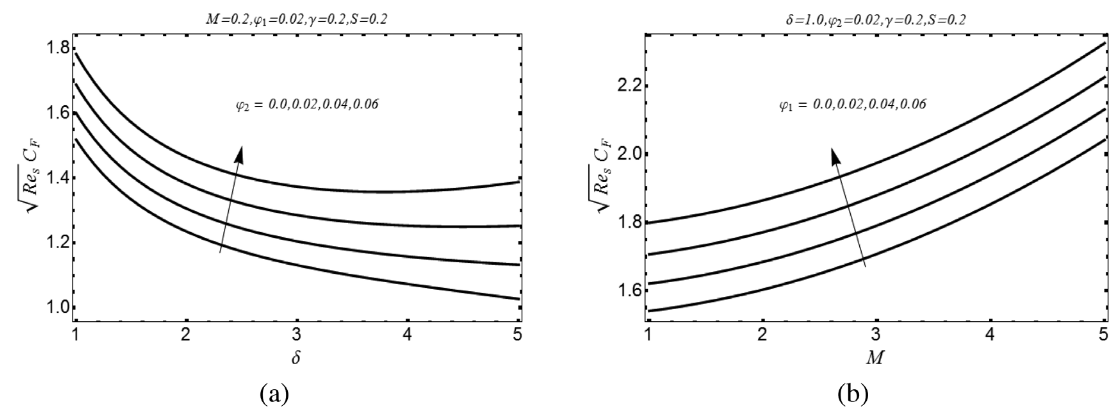

FIGURE 8 Variation in skin friction coefficient $\sqrt{Re_x}C_F$.

of $(\delta), (\varphi_1), (\varphi_2), (\lambda)$ and (θ_w). However, it shows decreasing response with rising values of (Pr) and thermal slip parameter (Γ). This is because the Prandtl number depicts an inverse relationship with thermal diffusivity. As a consequence, thermal diffusivity shows a reducing manner with boosting values of the Prandtl number. That's why the temperature profile and the concerned thermal boundary layer thickness of the hybrid nanofluid show a diminishing response with an upward value of the Prandtl number (Pr).

The alteration in amplitude of coefficient of skin friction $(\sqrt{\mathrm{Re}_x}C_F)$ for interval $\tau \in [0, 10\pi]$ is demonstrated in Figures 7a–d. These figures clarify that $(\sqrt{\mathrm{Re}_x}C_F)$ amplitude is enhanced by mounting (φ_1), (φ_2) and (S), and diminishes with (γ). Figure 8a,b illustrates the outcomes of (φ_2) versus (δ) and (φ_1) versus (M) on $(\sqrt{\mathrm{Re}_x}C_F)$ when $\tau = \pi/2$ fixed. It is viewed that the profile $(\sqrt{\mathrm{Re}_x}C_F)$ shows declining behavior with (δ). However, it enhances with upward values of (φ_1), (φ_2), and (M).

5 | CONCLUSIONS

The current investigation evaluated the influences of velocity and thermal slip, and nonlinear thermal radiation in a magnetohydrodynamic hybrid nanofluid towards an oscillating stretched curved surface. HAM is executed to calculate the series solution of the established flow equations. The subsequent note-worthy results that have been witnessed from recent exploration are depicted as

- The amplitude of liquid velocity depicts boosting manner with mounting values of (φ_1), whilst it diminishes for (δ), (φ_2) and (γ).
- At $\tau = \pi/2$, the liquid velocity profile reduces with growing (φ_2) and (γ). However, it inclines for (δ) and (φ_2).
- The temperature and the connected boundary layer thickness are rises for the advanced values of (δ), (φ_1), (θ_w), (λ) and φ_2.While, its temperature drops with rising (Γ) and (Pr).
- For mounting values of (φ_1), (δ), (S) and (φ_2), the amplitude of $P(\xi, \tau)$ is decreased.
- At time instant $\tau = \pi/2$, the pressure distribution profile $P(\xi, \tau)$ shows a reducing response with elevated values of the velocity slip parameter (γ). However, it shoot upwards for the solid volume fraction variable for alumina (φ_1), the non-dimensional variable of radius of curvature (δ) and the solid volume fraction variable for copper (φ_2).
- The amplitude of $\sqrt{Re_x} C_F$ rises for developed values of (φ_1), (φ_2) and (S), whereas it decays by increasing (γ).
- The magnitude of the skin friction coefficient $\sqrt{Re_x} C_F$ at $\tau = \pi/2$ is a mounting function of the parameters of the solid volume fraction variable for alumina (φ_1), the magnetic parameter (M), and the solid volume fraction variable for copper (φ_2).Whilst for boosting values of (δ), it shows opposite trend.
- The magnitude of $Nu_x/\sqrt{\mathrm{Re}_x}$ upshots with (φ_2), (λ), (Pr) and (θ_w). However, with improved values of (Γ), (φ_1) and (δ), it reduces.

NOMENCLATURE

α	stretching rate (s^{-1})
B_0	strength of magnetic field
$(c_p)_{hnf}$	specific heat capacity of hybrid nanofluid $(J/Kg\mathrm{K})$
C_1	radius of curvature
C_F	dimensionless Coefficient of skin friction
F_ξ	non-dimensional velocity
k_{hnf}	thermal conductivity of the hybrid nanoliquid $(W/m^{-2}\mathrm{K})$
ℓ_1	velocity slip parameter
ℓ_2	thermal slip parameter
M	magnetic parameter
n_f	nanofluid
h_{nf}	hybrid nanofluid
Nu_x	non-dimensional local Nusselt number
p	pressure of the fluid
P	dimensionless pressure
Pr	Prandtl number
$\widehat{q}_r$	radiative heat flux
x	axial directional coordinate of the curved surface
S	Relation of oscillatory frequency of the surface to stretching rate constant
s_1	solid component for alumina
s_2	solid component for copper
t	time (s)
T	temperature of the fluid (K)
T_w	temperature of the oscillatory surface (K)
T_∞	ambient fluid temperature (K)
r	normal direction to the curved surface (m)
u_1	component of velocity along radial r- direction (m/s)
v_1	component of velocity along axial x- direction (m/s)

Greek letter

α_f	thermal diffusivity of the base fluid
Γ	dimensionless thermal slip parameter
γ	dimensionless velocity slip parameter
λ	dimensionless radiation parameter
δ	dimensionless radius of curvature
ξ	dimensionless similarity variable
ν_f	kinematic viscosity of the base fluid (m/s^2)
μ_{hnf}	Viscosity of the hybrid nanoliquid (kg/ms^2)
σ_{hnf}	electrical conductivity of hybrid nanoliquid (Sm^{-1})
ρ_{hnf}	density of hybrid nanoliquid (kg/m^3)
ϖ	angular frequency (s^{-1})
θ	dimensionless fluid temperature
θ_w	dimensionless temperature parameter
φ_1	parameter of solid volume fraction for alumina
φ_2	parameter of solid volume fraction for copper

ACKNOWLEDGMENTS
We are thankful to the worthy reviewers for their encouraging comments and productive suggestions to increase the quality of the manuscript.

CONFLICT OF INTEREST STATEMENT
I and all the coauthors have no conflict in submitting the manuscript.

ORCID
Muhammad Imran https://orcid.org/0000-0002-2760-3595
Muhammad Naveed https://orcid.org/0000-0002-9616-3087
Babar Iftikhar https://orcid.org/0000-0001-9852-8265
Zaheer Abbas https://orcid.org/0000-0002-1300-7098

REFERENCES
[1] Choi, S.U.S.: Enhancing thermal conductivity of fluids with nanoparticle. ASME Int. Mech. Eng. Congress Exp. 66, 99–105 (1995)
[2] Hayyat, T., Kiran, A., Imtiaz, M., Alsaedi, A.: Hydromagnetic mixed convection of copper and silver water nanofluids due to a curved stretching sheet. Results Phys. 6, 904–910 (2016)
[3] Hayat, T., Rashid, M., Alsaedi, A., Ahmed, B.: Flow of nanofluid by nonlinear stretching velocity. Results Phys. 8, 1104–1109 (2018)
[4] Abbas, Z., Imran, Z., Naveed, M.: Impact of equally diffusive chemical reaction on time-dependent flow of casson nanofluid due to oscillatory curved stretching surface with thermal radiation. Arab. J. Sci. Eng. 47, 16059–16078 (2022)
[5] Farooq, U., Hayat, T., Alsaedi, A., Liao, S.J.: Series solutions of non-similarity boundary layer flows of nano-fluids over stretching surfaces. Numer. Algorithms. 70, 43–59 (2015)
[6] Farooq, U., Zhi-Liang, L.: Nonlinear heat transfer in a two-layer flow with nanofluids by OHAM. J. Heat Transf. 1(2), 136 (2014)
[7] Lu, D.C., Farooq, U., Hayat, T., Rashidi, M.M., Ramzan, M.: Computational analysis of three layer fluid model including a nanomaterial layer. Int. J. Heat Mass Transf. 122, 222–8 (2018)
[8] Cui, J., Azam, F., Farooq, U., Hussain, M.: Non-similar thermal transport analysis in entropy optimized magnetic nanofluids flow by considering effective Prandtl number model with melting heat transfer and Joule heating. J. Magn. Magn. Mater. 567, 170331 (2023)
[9] Sagheer, S., Farooq, U., Hussain, M.: Non-similar investigation of enhanced thermal efficiency of Maxwell based hybrid nanofluid (MoS2+ ZnO) across a linearly stretched surface. J. Magn. Magn. Mater. 565, 170285 (2023)
[10] Cui, J., Tahir, K., Farooq, U., Hussain, M., Ali, C.J.: Non-similar mixed convection analysis for magnetic flow of Williamson nano-fluid over vertically stretching surface subjected to viscous dissipation, porous media and heat sou. J. Porous Media. 26(7), 103–119 (2023)
[11] Waini, I., Ishak, A., Pop, I.: Flow and heat transfer along a permeable stretching/shrinking curved surface in a hybrid nanofluid. Phys. Scr. 94(10), 105219 (2019)
[12] Nadeem, S., Abbas, N., Malik, M.Y.: Inspection of hybrid based nanofluid flow over a curved surface. Comp. Meth. Prog. Biomed. 189, 105193 (2020)
[13] Saeed, A., Alghamdi, W., Mukhtar, S., et al.: Darcy-Forchheimer hybrid nanofluid flow over a stretching curved surface with heat and mass transfer. PLoS One. 16(5), e0249434 (2021)

[14] Naveed, M., Ali, S., Hasnain, J., et al.: Analysis of Joule heating and Hall current on flow of hybrid nanofluid over a curved stretching surface with melting boundary condition. Heat Transf. Res. 52(5), 1–16 (2021)

[15] Mahdy, A., El-Zahar, E.R., Rashad, A.M., Saad, W., Al-Juaydi, H.S.: The magneto-natural convection flow of a micropolar hybrid nanofluid over a vertical plate saturated in a porous medium. Fluids 6(6), 202 (2021)

[16] El-Zahar, E.R., Rashad, A.M., Al-Juaydi, H.S.: Studying massive suction impact on magneto-flow of a hybridized Casson nanofluid on a porous continuous moving or fixed surface. Symmetry. 14(3), 627 (2022)

[17] Shaik, J., Polu, B.A., Ahmed, M.M., Rashad, A.M.: Characteristics of moving hot block and non-Fourier heat flux model on sinusoidal wavy cavity filled with hybrid nanofluid. Eur. Phys. J. Plus. 137(1), 131 (2022)

[18] Rashad, A.M., Nafe, M.A., Eisa, D.A.: Heat generation and thermal radiation impacts on flow of magnetic Eyring–Powell hybrid nanofluid in a porous medium. Arab. J. Sci. Eng. 48(1), 939–52 (2023)

[19] Ahmed, S.E., Reddy, P.B., Jakeer, S., Rashad, A.M., Salah, T.: Magnetic convection-radiation interaction in wavy porous triangular containers using hybrid nanofluids: Entropy analysis. J. Porous Media 26(5), (2023)

[20] Crane, L.J.: Flow past a stretching plate, Zeitschrift Fur Angew. Math. Und Phys. ZAMP. 21, 645–647 (1970)

[21] Sajid, M., Ali, N., Javed, T., et al.: Stretching a curved surface in a viscous fluid. Chin. Phys. Lett. 27, 024703 (2010)

[22] Naveed, M., Abbas, Z., Zia, Q.M., et al.: Analysis of heat transfer of hydromagnetic flow over a curved generalized stretching or shrinking surface with convective boundary condition. Therm. Sci. 23(6), 3775–3783 (2019)

[23] Sanni, K.M., Hussain, Q., Asghar, S.: Heat transfer analysis for non-linear boundary driven flow over a curved stretching sheet with a variable magnetic field. Front. Phys. 8, 113 (2020)

[24] Shi, Q.H., Shabbir, T., Mushtaq, M., et al.: Modelling and numerical computation for flow of micropolar fluid towards an exponential curved surface: a Keller box method. Sci. Rep. 11(1), 1–13 (2021)

[25] Khan, S.U., Shehzad, S.A., Nasir, S.: Unsteady flow of chemically reactive Oldroyd-B fluid over oscillatory moving surface with thermo-diffusion and heat absorption/generation effects. J. Braz. Soc. Mech. Sci. Eng. 41(2), 72 (2019)

[26] Abbas, Z., Imran, M., Naveed, M.: Time-dependent flow of thermally developed viscous fluid over an oscillatory stretchable curved surface. Alex. Eng. J.. 59(6), 4377–4390 (2020)

[27] Imran, M., Abbas, Z., Naveed, M., et al.: Impact of Joule heating and melting on time-dependent flow of nanoparticles due to an oscillatory stretchable curved wall. Alex. Eng. J. 60(4), 4097–4113 (2021)

[28] Naveed, M., Imran, M., Abbas, Z.: Curvilinear flow of micropolar fluid with Cattaneo–Christov heat flux model due to oscillation of curved stretchable sheet. Z. Naturforsch. A. 76(9), (2021)

[29] Imran, M., Abbas, Z., Naveed, M.: Flow of Eyring-Powell liquid due to oscillatory stretchable curved sheet with modified Fourier and Fick's model. Appl. Math. Mech. 42(10), 1461–1471 (2021)

[30] Naveed, M., Abbas, Z., Imran, M.: Analytical simulation of time dependent electromagneto-hydrodynamic flow of Williamson fluid due to oscillatory curved convectively heated Riga surface with variable thermal conductivity and diffusivity. J. Process Mech. Eng. 0(0), 1–16, (2021)

[31] Naveed, M., Imran, M., Gul, S.: Heat transfer analysis in hydromagnetic flow of couple stress fluid in presence of homogeneous and heterogeneous chemical reactions over a porous oscillatory stretchable sheet. Adv. Mech. Eng. 15(2), 16878132231155823 (2023)

[32] Imran, M., Naveed, M., Abbas, Z.: Dynamics of Soret and Dufour effects on oscillatory flow of couple stress fluid due to stretchable curved surface. Adv. Mech. Eng. 15(2), 16878132231156742 (2023)

[33] Abbas, Z., Imran, M., Naveed, M.: Hydromagnetic flow of Carreau fluid in a curved Channel with non-linear thermal radiation, Therm. Sci. 23(6A), 3379–3390 (2019)

[34] Naveed, M., Imran, M., Akhter, S., et al.: Dynamics of melting heat transfer in thermally developed and chemically reactive flow of Eyring-Powell liquid through a curved channel. Rev. Mat. 72, 299–316 (2023)

[35] Naveed, M., Imran, M., Abbas, Z., et al.: Analysis of entropy generation and Joule heating on curvilinear flow of thermally radiative viscous fluid due to an oscillation of curved Riga surface. Int. J. Mod. Phys. C 33(07), 2250087 (2022)

[36] Abbas, Z., Naveed, M., Sajid, M.: Hydromagnetic slip flow of nanofluid over a curved surface. J. Mol. Liq. 216, 756–762 (2015)

[37] Meenakumari, R., Lakshminarayana, P., Vajravelu, K.: Influence of induced magnetic field and slip conditions on convective Prandtl fluid flow over a stretching surface with homogeneous and heterogeneous reactions. Multidiscip. Model. Mater. Struct. 17(1), 127–147 (2020)

[38] Wahid, N.S., Hafidzuddin, M.E.H., Arifin, N., et al.: Magnetohydrodynamic (MHD) slip Darcy flow of viscoelastic fluid over a stretching sheet and heat transfer with thermal radiation and viscous dissipation. CFD Lett. 12(1), 1–12 (2020)

How to cite this article: Imran, M., Naveed, M., Iftikhar, B., Abbas, Z.: Heat transfer analysis in a curvilinear flow of hybrid nanoliquid across a curved oscillatory stretched surface with nonlinear thermal radiation. Z Angew Math Mech. e202200600 (2023). https://doi.org/10.1002/zamm.202200600